Journal of Proteomics 128 (2015) 333–343

Contents lists available at ScienceDirect

Journal of Proteomics

journal homepage: www.elsevier.com/locate/jprot

Proteomic analysis of the crayfish gastrolith chitinous extracellular matrix reveals putative protein complexes and a central role for GAP 65

Lilah Glazer [a,1,2], Ziv Roth [a,2], Simy Weil [a], Eliahu D. Aflalo [a], Isam Khalaila [b], Amir Sagi [a,*]

[a] Department of Life Sciences and The National Institute for Biotechnology in the Negev, Ben-Gurion University of the Negev, Beer-Sheva, Israel
[b] Department of Biotechnological Engineering, Ben-Gurion University of the Negev, Beer-Sheva, Israel

ARTICLE INFO

Article history:
Received 20 July 2015
Received in revised form 17 August 2015
Accepted 24 August 2015
Available online 28 August 2015

Keywords:
Chitin
Crayfish
Extracellular matrix
Gastrolith
Gastrolith matrix proteins (GMPs)
Protein complex

ABSTRACT

Chitin is a major component of arthropod cuticles, where it forms a three-dimensional network that constitutes the scaffold upon which cuticles form. The chitin fibers that form this network are closely associated with specific structural proteins, while the cuticular matrix contains many additional structural, enzymatic and other proteins. We study the crayfish gastrolith as a simple model for the assembly of calcified cuticular structures, with particular focus on the proteins involved in this process. The present study integrates a gastrolith-forming epithelium transcriptomic library with data from mass spectrometry analysis of proteins extracted from the gastrolith matrix to obtain a near-complete picture of gastrolith protein content. Using native protein separation we identified 24 matrix proteins, of which 14 are novel. Further analysis led to discovery of three putative protein complexes, all containing GAP 65 the most abundant gastrolith structural protein. Using immunological methods we further studied the role of GAP 65 in the gastrolith matrix and forming epithelium, as well as in the newly identified protein complexes. We propose that gastrolith matrix construction is a sequential process in which protein complexes are dynamically assembled and disassembled around GAP 65, thus changing their functional properties to perform each step in the construction process.

Biological significance: The scientific interest on which this study is based arises from three main features of gastroliths: (1) Gastroliths possess partial analogy to cuticles both in structural and molecular properties, and may be regarded, with the appropriate reservations (see Introduction), as simple models for cuticle assembly. At the same time, gastroliths are terminally assembled during a well-defined period, which can be controlled in the laboratory, making them significantly easier to study than cuticles. (2) Gastroliths, like the crayfish exoskeleton, contain stable amorphous calcium carbonate (ACC) rather than crystalline calcite. The biological mechanism for the stabilization of a naturally unstable, but at the same time biologically highly available, calcium carbonate polymorph is of great interest from the pharmaceutical point of view. (3) The gastrolith organic matrix is based on a highly structured chitin network that interacts with a variety of substances. This biologically manipulated, biodegradable structure is in itself of biotechnological and pharmaceutical potential. A growing body of evidence indicates that proteins play central roles in all above aspects of gastrolith construction.

This study offers the first comprehensive screening of gastrolith proteins, and we believe that the analysis presented in this work can not only help reveal basic biological questions regarding assembly of mineralized and non-mineralized cuticular structures, but may also serve as basis for applied research in the fields of agriculture (e.g. cuticle-based pest management), health (e.g. bioavailable calcium supplements and biodegradable drug carriers) and materials science (e.g. non-toxic scaffolds for water purification).

1. Introduction

Chitin, the second-most abundant polysaccharide in nature after cellulose, is a major component of arthropod cuticles, where it is assembled into three-dimensional networks that serve as light but mechanically strong scaffolds [1,2]. While it is known that cuticular chitin is assembled by the enzyme chitin synthetase [3], the specific mechanism by which chitin is produced remains unknown. Available evidence suggests that chitin is synthesized by membrane-bound clusters of chitin synthase catalyzing the formation of linear chains consisting of β-(1 → 4) linked *N*-acetyl-D-glucosamine (GlcNAc)

Abbreviations: ACC, amorphous calcium carbonate; CqCBP, *C. quadricarinatus* chitin-binding protein; CqCc1, *C. quadricarinatus* cryptocyanin 1; GFE, gastrolith-forming epithelium; GMPs, gastrolith matrix proteins; LPS-BP, lipopolysaccharide and beta-1,3-glucan-binding protein; LEA, late embryogenesis abundant; NGS, next-generation sequencing.

* Corresponding author at: Department of Life Sciences and The National Institute for Biotechnology in the Negev, Ben-Gurion University of the Negev, Beer-Sheva 84105, Israel.
E-mail addresses: lglazer@whoi.edu (L. Glazer), isam@bgu.ac.il (I. Khalaila), sagia@bgu.ac.il (A. Sagi).
[1] Present address: Biology Department, Woods Hole Oceanographic Institution, Woods Hole, MA, USA.
[2] Equally contributed the major part of the study.

http://dx.doi.org/10.1016/j.jprot.2015.08.016
1874-3919/

subunits. These chains are then translocated across the plasma membrane to the extracellular matrix, where they assemble into crystalline microfibrils via interchain hydrogen bonding. Subsequent association with cuticular proteins and the formation of an ordered network of cross-linked fibers ensue [1,4–7]. Cuticular proteins are long recognized as serving many different roles, including chemical modification of the chitin microfibrils [8], remodeling of the chitin network [9], immunological defense [10], pigmentation [11–14] and cross-linking of chitin microfibrils in a process called sclerotization [15,16].

In the exoskeletons of most crustaceans, cuticular sclerotization is followed by the deposition of minerals, namely calcium carbonate [7,17], as an additional hardening factor. Calcium carbonate is deposited either as the crystalline form of calcite, or as stable ACC [7]. ACC is a naturally unstable form of calcium carbonate, and substantial evidence has shown that in the crustacean exoskeleton, this compound is stabilized through the involvement of proteins and/or peptides [18,19] as well as organic and inorganic molecules and ions [20–23].

Exoskeleton formation is a cyclical process performed periodically as the animal grows and molts. During each molt event, there is formation of a new cuticular chitin–protein structure, which in crustaceans also corresponds with a calcification process. To generate a new exoskeleton, crayfish rely on gastroliths, cuticle-like structures that serve as temporary calcium storage organs, and assist in the fast hardening of the new post-molt cuticle [18,24]. Gastroliths are formed in an enclosed pouch found between the gastrolith-forming epithelium and the cuticular stomach wall [25]. Like the exoskeleton, gastroliths are composed of an organic matrix consisting of chitin and proteins, with precipitated mineral in the specific form of ACC [17]. The resemblance between gastroliths and the exoskeleton can be seen not only in terms of ultrastructure but also in transcript expression and protein content [19,26,27]. On the other hand, gastroliths lack some of the structural complexity of the exoskeleton [17,25,28] and are, therefore, considered as simple models that can be used to study certain aspects of exoskeleton structure and formation [12,29].

In our long-term study of crayfish gastrolith structure, composition and formation [12,17,19,27,29], one of our main goals has been to achieve as complete a picture of proteins participating in gastrolith formation as possible and to study potential interactions between them. So far, three proteins, namely GAMP from the gastroliths of the crayfish *Procambarus clarkii* [30–32], and GAP 65 and GAP 10, from the gastroliths of the crayfish *Cherax quadricarinatus* [19,27], have been identified as being expressed in the gastrolith-forming epithelium and secreted to the gastrolith matrix. All three predicted protein sequences were obtained through the use of mass spectrometric peptide sequencing for directing the synthesis of degenerate primers, followed by PCR amplification and sequencing of the responsible transcripts. In some cases, the process was aided by the generation of cDNA libraries from relevant tissues. A fourth deduced protein, CqCDA1, was identified based on the detection of significant up-regulation of its transcript during pre-molt in the gastrolith-forming epithelium in a microarray analysis of pre-molt versus intermolt transcript levels [26].

In 2012, we suggested a structural model assigning specific roles for these four proteins and predicting the participation of additional, yet to be identified, proteins in gastrolith formation [12]. Our model was based on the division of gastrolith proteins into three functional groups: (1) proteins that are exclusively involved in construction of the chitinous matrix, (2) proteins that are directly involved in the precipitation of the ACC and that have no direct association with chitin, and (3) proteins that participate in both processes (i.e. multi-task proteins). The above-mentioned gastrolith proteins were assigned to the appropriate group based on sequence analysis and other published empirical data. In addition to assigning potential functions, we suggested the existence of protein–protein interactions involved in the formation of gastrolith protein complexes necessary for attachment of non-chitin-binding proteins to the organic matrix, as well as for other purposes. However, additional information on gene expression in the gastrolith-forming epithelium and on protein sequences from the gastrolith matrix to identify such interactions was not available at the time.

In recent years, protein biochemistry studies have reached the level of high throughput largely due to advances made in tandem mass spectrometry technology [33,34]. Next-generation sequencing (NGS)-generated transcriptomic libraries can be used as databases for such MS-based studies [29], especially when studying a biological system responsible for the assembly of a well-defined construct in a specialized tissue. The crayfish gastrolith offers an ideal platform for applying this strategy, in addition to being a good model for studying exoskeleton formation. Accordingly, we recently employed the NGS method of 454-sequencing to obtain a transcriptome of *C. quadricarinatus* epithelial tissues [29]. The RNA samples were extracted from the gastrolith-forming and sub-cuticle epithelia at four molt stages, i.e. intermolt, early pre-molt, late pre-molt and post-molt.

In the present study, we have made use of this comprehensive epithelial library to complement protein biochemistry efforts aimed at cataloging those proteins incorporated into *C. quadricarinatus* gastroliths. In doing so, several novel proteins were identified. In addition, we present evidence for the existence of three dominant protein complexes within the gastrolith, and identify the putative protein composition of each suspected complex. We further found that GAP 65 is present in each complex. On the basis of this last finding together with evidence from immunostaining experiments detecting GAP 65 distribution and localization in the gastrolith-forming epithelium (GFE) and gastrolith matrix, we propose that GAP 65 serves as a central protein in the identified protein complexes.

2. Materials and methods

2.1. Animals and molt

C. quadricarinatus males were grown in artificial ponds at Ben-Gurion University of the Negev, Beer-Sheva, Israel, under conditions described in Shechter et al. [17]. Inter-molt crayfish were held in individual cages and endocrinologically induced to enter pre-molt through removal of the X organ-sinus gland (XO-SG) complex or repeated ecdysone injection. Progression of the molt cycle was monitored daily by measuring the gastrolith molt mineralization index (MMI), as described by Shechter et al. [35]. For all dissection procedures, crayfish were placed on ice for 10–15 min, until anesthetized.

2.2. Immunodetection of GAP 65 in the gastrolith matrix and gastrolith-forming epithelium by fluorescence microscopy

For immunohistochemistry, whole gastrolith pouches were submerged in a decalcifying fixative containing 7% EDTA and 0.2% glutaraldehyde in 0.1 M phosphate-buffered saline (PBS). Alternatively, an isolated GFE was submerged in 4% formaldehyde in PBS, dehydrated in ethanol and embedded in paraffin. Paraffin sections (5 μm-thick) were deparaffinized, rehydrated, incubated in 0.5 M citrate buffer, pH 6.0 (30 min at 95 °C) for antigen retrieval and washed in 0.01 M PBS, pH 7.4. Blocking with 2% normal goat serum, 0.1% Triton X-100, and 0.05% Tween 20 in PBS was performed for 1 h at room temperature (RT), followed by incubation with rabbit polyclonal anti-GAP 65 antisera as primary antibodies (1:1000, v/v). The slides were washed in PBS and incubated with secondary goat anti-rabbit FITC conjugated antibodies (1:250 in PBS containing 0.2% fish skin gelatin) for 1 h at RT. After PBS washes, the slides were mounted (DAPI 1:1000 in PBS and 50% glycerol) and imaged using a fluorescence microscope.

2.3. GFE ultrastructure analysis by transmission electron microscopy (TEM)

GFEs were excised from late pre-molt animals and fixed in 2% glutaraldehyde in 0.2 M phosphate buffer (PB) pH 6.8, at RT for 1 h. The specimens were then fixed on ice for 1 h in a second fixative comprising of

1% glutaraldehyde and 1% osmium tetraoxide (OsO_4) in cold 0.2 M PB, pH 6.2, washed three times in cold water (30 min each) and incubated in 1% uranyl acetate overnight at 4 °C. This was followed by dehydration in a 30–100% acetone series (10% increments, 15 min each) and embedding in araldite resin, as follows: The specimens were rinsed twice in propylene oxide for 15 min each time, once in a 2:1 solution of propylene oxide and araldite for 15 min, once in a 1:1 solution of propylene oxide and araldite for 30 min, and overnight in a 1:2 propylene oxide and araldite mixture at 4 °C. The tissues were then transferred to araldite for 1 h, placed on pre-polymerized araldite blocks and embedded in araldite. These were then left at RT for 30 min, at which point the samples were oriented as desired and incubated at 60 °C for 24 h. Transverse sections were cut using a Leica UltraCut UCT ultramicrotome equipped with a diamond knife (Leica Microsystems UK), contrasted with uranyl acetate and lead citrate, and then examined using a Tecnai 12 G2 TWIN TEM (FEI) equipped with a Gatan 794 MultiScan CCD camera.

2.4. Immunolocalization of GAP 65 in the GFE

Electron microscopic immunolocalization of GAP 65 in the GFE was performed by cryo-sectioning [36] and immunolabeling. Briefly, GFEs were excised from late pre-molt animals and immediately fixed in 4% formaldehyde and 0.2% glutaraldehyde in 0.1 M PBS (prepared fresh) at 4 °C for 3 h, followed by several washes in 0.1 M PB at RT. The tissue was then cut into small rectangular pieces (length and width, ~2–3 mm each), soaked briefly in diluted bromophenol blue, washed several times in 0.1 M PB, and cryo-protected by immersion in 2.3 M sucrose in PBS in 1.5 ml vials at 4 °C overnight with slow rotation. Tissue pieces were mounted onto pins, and plunge-frozen in liquid nitrogen. Ultrathin cryosections (80–100 nm) were cut using a Leica UltraCut UCT Ultramicrotome equipped with low temperature sectioning system (Leica Microsystems UK), and collected on formvar-carbon-coated nickel grids. The cryo-sections were immunolabeled with rabbit polyclonal anti-GAP 65 (1:400–800) and goat anti-rabbit IgG (1:20–40) conjugated to 12 nm gold (Jackson ImmunoResearch Laboratories, West Grove, PA), followed by fixation with 1% glutaraldehyde in PBS. Finally, contrast enhancement and mounting were achieved with 2% uranyl acetate (pH 7) and a 1:9 ratio of 4% uranyl acetate and 2% methyl cellulose, followed by overnight drying of the grids at RT. Sections were viewed using a Tecnai 12 G2 TWIN TEM equipped with a Gatan 794 MultiScan CCD camera.

2.5. Purification of gastrolith matrix proteins and separation of GAP 65

Gastroliths were dissected from induced pre-molt crayfish, washed with distilled water and cleaned from remaining organic material by scraping the surface using an electrical grinder. The gastroliths were then ground to powder in liquid nitrogen. Extraction of gastrolith matrix proteins (GMPs) and separation of GAP 65 were performed following the procedure detailed in Shechter et al. [19]. Briefly, EGTA-extracted proteins were separated by HPLC on a DEAE column. Washes with a 0.1–1 M NaCl step gradient (0.1 M increments) were performed. The fraction collected at 1 M contained the purified and enriched GAP 65.

2.6. Separation of gastrolith matrix proteins by native PAGE

GMPs were incubated in Laemmli [37] sample buffer (without SDS and DTT) and resolved by native PAGE (4–20% gradient) (GeBAGel horizontal electrophoresis system, GEBA, Israel) with Tris-glycine buffer lacking SDS. The resulting bands were visualized by Coomassie brilliant blue (CBB) staining, excised from the gel and analyzed by tandem mass spectrometry, as described below.

2.7. Protein cross-linking and 2D electrophoretic separation of protein complexes

To identify protein complexes, protein cross-linking was performed using formaldehyde (FA) as described by Sutherland et al. [38]. Two hundred micrograms of GMPs were incubated with 1% formaldehyde for 30 min at 37 °C. Cross-linking was terminated upon incubation in glycine buffer (final concentration: 0.025 M, pH 8) for 15 min. A control sample was incubated in the same conditions without formaldehyde. Both the cross-linking products and the control sample were incubated in sample buffer for 30 min at 30 °C and resolved by non-reducing SDS-PAGE in the first dimension to resolve protein complexes. Lanes containing the cross-linking and the control samples were excised, separately transferred to 15 ml Falcon tubes and incubated in sample buffer for 45 min at 80 °C to reverse the cross-linking. Each lane was subsequently placed horizontally onto the top of a reducing SDS-PAGE gel to resolve each complex into its protein components. After separation in the 2nd dimension, bands were visualized by CBB staining.

2.8. GAP 65 biotinylation and avidin-based precipitation

Biotinylation of GAP 65 was performed using EZ-Link HPDP-Biotin (Thermo Fisher Scientific, San Jose, CA), according to the manufacturer's protocol. Briefly, 2 mg of GAP 65 were dissolved in PBS and incubated with 0.4 mM HPDP-biotin for 2 h at RT. Unbound biotin was removed using Vivaspin concentrating devices (Sartorius), with PBS as washing buffer. For avidin-agarose precipitation (co-AP) of GAP 65-interacting proteins, 100 μg of GMPs was incubated with 30 μg of biotinylated-GAP 65 for 2 h at RT in modified Tris buffer (Tris-buffered saline (TBS), 0.3% Triton X-100, 0.005 M $CaCl_2$ and 0.002 M 4-(2-aminoethyl) benzenesulfonyl fluoride (AEBSF)-hydrochloride (AppliChem)). Thirty microliters of agarose-bound avidin (high capacity neutravidin-agarose resin, Thermo Fisher Scientific) was added to the solution, which was incubated with agitation for an additional hour at RT. The solution was then centrifuged for 2 min at 8000 *g*. The supernatant was collected, and the pellet was washed thrice in modified Tris buffer and collected by centrifugation (2000 *g*, 1 min). The avidin-bound proteins were eluted by boiling in sample buffer and resolved on SDS-PAGE. The CBB-stained bands were excised and analyzed by tandem mass spectrometry.

2.9. Mass spectrometry

Reduction, alkylation and trypsinization steps were carried out as described previously [39]. For protein identification, peptides were loaded onto a homemade column (15 cm long, 75 μm internal diameter fused silica) packed with Jupiter C-18 300 Å, 5 μm beads (Phenomenex) and connected to an Eksigent nano-LC system (Eksigent, Dublin, CA). Elution was performed with two solutions, namely solvent A (2% acetonitrile in 0.1% formic acid) and solvent B (80% acetonitrile in 0.1% formic acid), via a linear gradient (5–65%) created by solvent B over 45 min. MS peptide analysis and tandem MS fragmentation were performed using the LTQ-Orbitrap (Thermo Fisher Scientific). The mass spectrometer was operated in the data-dependent mode to enable switching between MS and collision-induced dissociation tandem MS analyses of the top eight ions. Collision-induced dissociation fragmentation was performed at 35% collision energy with a 30 ms activation time. Proteins were identified and validated using the SEQUEST algorithm operated under the Proteome Discoverer 1.3 software (Thermo Fisher Scientific) and a 454-based *C. quadricarinatus* epithelial transcript library [29]. Mass tolerance for precursors and fragmentations was set to 10 ppm and 0.8 Da, respectively. Only proteins containing at least two peptides of high confidence (Xcore > 2 or 2.5 for doubly or triply charged species, respectively) were chosen.

2.10. Bioinformatics analyses

Deduction of amino acid sequences of the entire *C. quadricarinatus* epithelial transcript library (GADE01000000) was performed using the ORF-predictor server [40]. Signal peptides were predicted using SignalP 3.0, part of the CBS Prediction Servers suite (http://www.cbs.dtu.dk/services/SignalP). General domain analyses were performed using SMART [33,41]. Pair alignments were performed using the LALIGN algorithm [42]. Amino acid compositions were analyzed using the ProtParam tool found as part of the ExPASy collection of programs (http://web.expasy.org/protparam).

2.11. Accession numbers

GenBank accession numbers were assigned to the following proteins: Gastrolith protein 59 (GAP 59), KP968827; chitinase 2, KP968828; beta-N-acetylglucosaminidase, KP968829; GAMP-like, KP968830; *C. quadricarinatus* chitin-binding protein (CqCBP), KP968831; gastrolith protein 18.2 (GAP 18.2), KP968832; gastrolith protein 02526 (GAP 02526), KP968833; *C. quadricarinatus* cryptocyanin 1 (CqCc1), KP968834; cyclophilin, KP968835; cystatin 1, KP968836; cystatin 2, KP968837; lipopolysaccharide and beta-1-3-glucan-binding protein (LPS-BP), KP968838; late embryogenesis abundant protein (LEA), KP968839; and crustacyanin A, KP968840.

3. Results and discussion

3.1. Immunodetection of GAP 65 in the gastrolith matrix and gastrolith-forming epithelium by fluorescence microscopy

GAP 65 is the most abundant protein in the gastrolith matrix [19]. As such, we undertook to examine GAP 65 distribution in cross-sections of partially decalcified gastrolith pouches and in cross-sections of the GFE using polyclonal anti-GAP 65 antibodies through immunohistochemistry (Fig. 1). Hematoxylin and eosin (H&E) staining (Fig. 1A, left image) revealed the lamellar structure of the gastrolith matrix formed by the chitin layers. Within the gastrolith matrix, GAP 65 was distributed along chitin layers that form the entire structure of the gastrolith (Fig. 1A, right image). In addition, the amount of GAP 65 immunostaining seemed to be higher in the inner region of the matrix that had undergone only partial decalcification, as opposed to the fully decalcified outer region (separated by dashed line in Fig. 1A, right image). This observation coincides with previous findings showing that GAP 65 is mostly extracted during gastrolith decalcification but that a fraction of the protein remains attached to the chitin during this process and requires stronger extraction conditions for its complete removal [12,19].

Fig. 1B shows that staining reflecting high levels of GAP 65 was detected in the cytoplasm but not the nuclei of cells constituting the GFE. In addition, the immunolabeling was also detected in the connective tissue linking the GFE and hemolymph.

Finally, to confirm the specificity of the immunolabeling, the assay was repeated using only the secondary antibodies. No signal was detected (Fig. S1).

3.2. Immunolocalization of GAP 65 in the gastrolith-forming epithelium by TEM

For closer examination of the epithelial cells and localization of GAP 65 therein, TEM was conducted (Fig. 2). We initially inspected cellular ultrastructure and observed the classical features of a secreting epithelium [43], including a basal side adjacent to the inner connective tissue and an apical side directed towards the gastrolith pouch. The basal side was enriched in nuclei (data not shown), while the apical side was lined

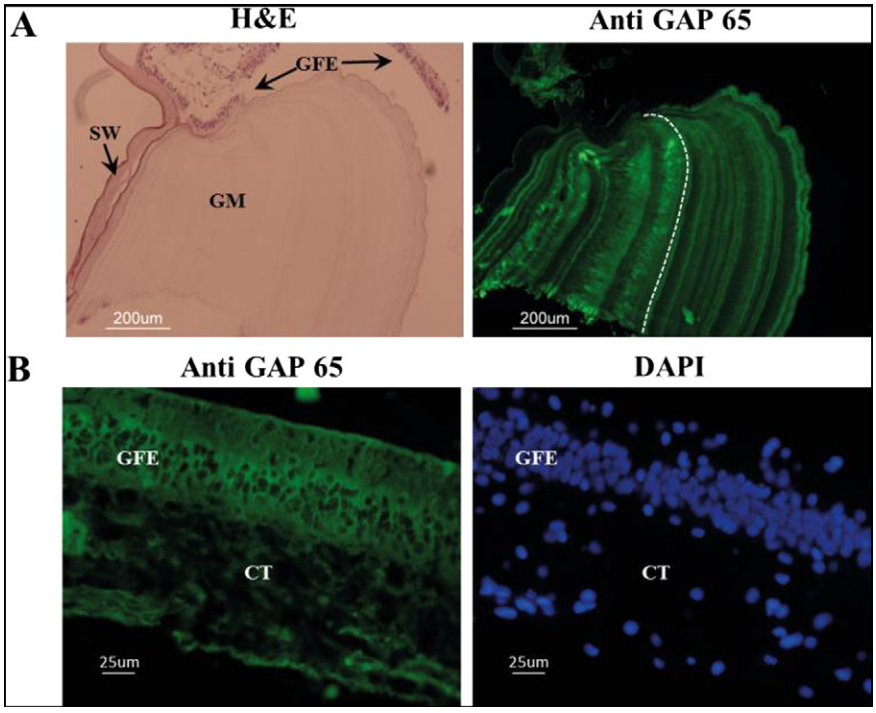

Fig. 1. Immunohistochemical detection of GAP 65 distribution throughout the gastrolith matrix and gastrolith-forming epithelium. A) In the left image, H&E staining of cross-sections of a partially decalcified gastrolith pouch. GFE, gastrolith-forming epithelium; GM, gastrolith matrix; SW, stomach wall. In the right image, GAP 65 is observed in the gastrolith matrix. The white dashed line differentiates the region of full decalcification (right of line) and partial decalcification (left of line). B) Left image: GAP 65 is observed in the cytoplasm of the GFE and adjacent connective tissue cells, all shown in cross-section. Right image: DAPI counter-staining served to identify nuclei in the GFE and connective tissue. CT, connective tissue. The protein was not observed in nuclei.

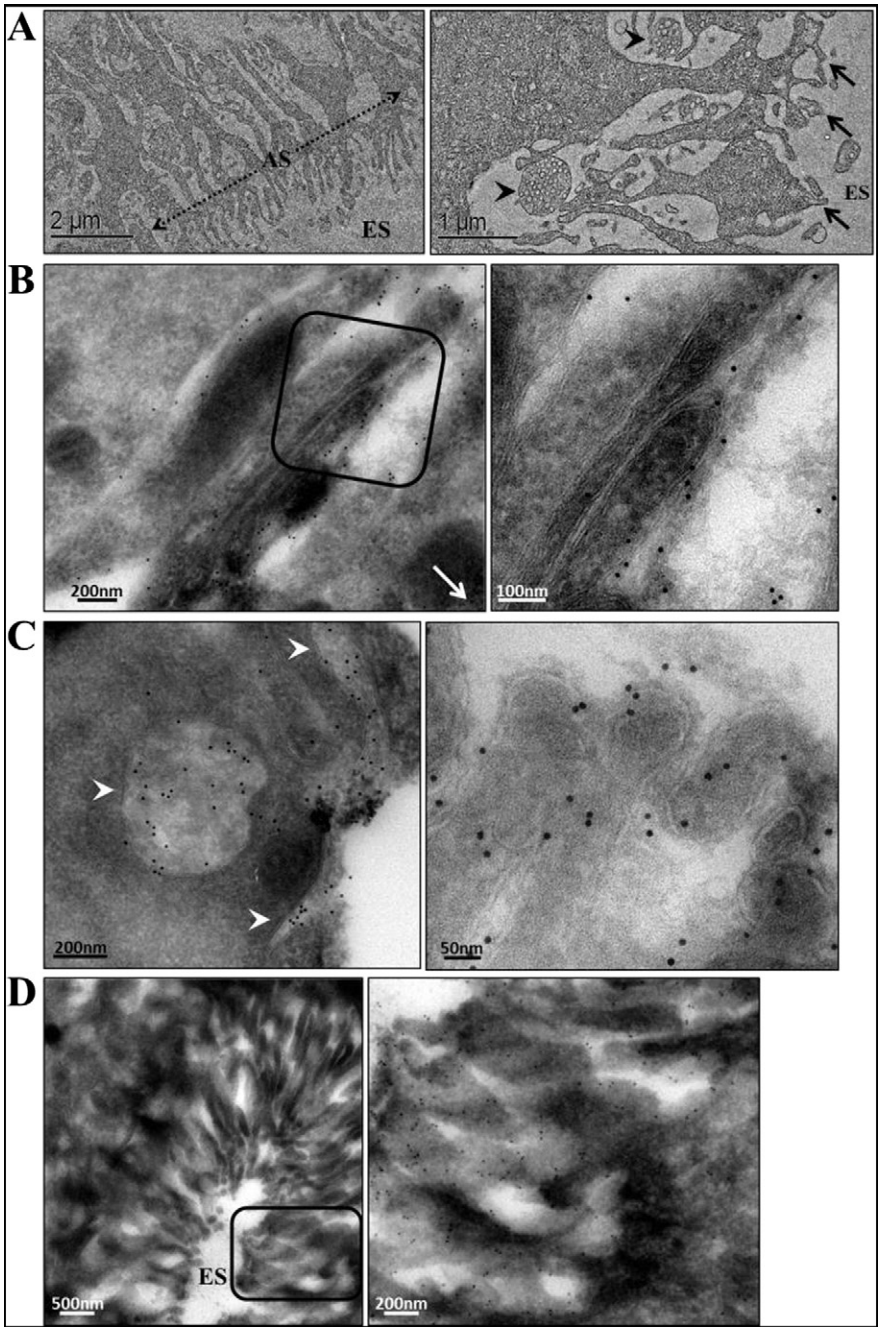

Fig. 2. Immunolocalization of GAP 65 in elements of the secretion pathway in the GFE. A) Ultrastructure of the apical face of the gastrolith-forming epithelium. Left image: The apical surface (AS, diagonal arrows) of the epithelium is characterized by numerous microvilli. Right image: Microvilli are indicated by arrows and structures suspected as exocytotic vesicles are indicated by arrowheads. B) Left image: GAP 65 is detected in membranes of the Golgi apparatus. White arrow indicates direction of apical surface. Right image: Magnification of the boxed area in the left image. C) Left image: GAP 65 is detected in exocytotic vesicles (arrowheads). Right image: Higher magnification of vesicles located at the apical edge of the cells, showing GAP 65 closely associated with vesicle membranes. D) Left image: GAP 65 labeling in microvilli. Right image: Magnification of the boxed area in the left image. ES, extracellular space.

with microvilli and enriched in secretion vesicles (Fig. 2A). Next, anti-GAP 65 antibodies were applied followed by gold-conjugated secondary antibodies to delineate GAP 65 localization within the epithelial cells. We found that GAP 65 is strongly associated with intracellular membranes, including concentrations of gold particles in what is apparently the Golgi complex (Fig. 2B), and in suspected secretion vesicles (Fig. 2C, left and right images). Scanning of microvilli found at the apical secreting edges of the epithelial cells revealed increased concentrations of gold labeling as compared to labeling seen in adjacent inner cell regions (Fig. 2D).

When only secondary antibodies were applied no gold labeling of the microvilli-rich apical area of GFE cells was detected (Fig. S2A). In addition, only sporadic gold particles were detected in hemocytes (Fig. S2B, left image) or nuclei (example in Fig. S2B, right image), structures that are unrelated to the epithelial secretion pathway, as opposed to numerous gold particles seen in the adjacent cytoplasm and membrane systems.

The TEM images support a scenario whereby GAP 65 is expressed and processed in the cells of the GFE, and secreted to the gastrolith pouch via vesicles. Indeed, GAP 65 is predicted to bear an N-terminal signal peptide directing it to the secretory pathway. GAP 65-containing vesicles could contain other proteins or chitin strands, although this has yet to be tested.

3.3. Identification of novel proteins and putative protein complex components in the gastrolith matrix

Based on the hypothesis that GAP 65 does not exert its varied range of effects [19] alone, our next step was to look for candidate proteins that potentially form associations with GAP 65 within the gastrolith matrix. For this, GMPs were separated on native-PAGE. Ten bands were detected (Fig. 3A, n1–10), excised from the gel and trypsin-digested. The peptides were subjected to MS analysis followed by search against our *C. quadricarinatus* epithelial transcript library [29]. In this manner, several proteins were identified in each band (Fig. 3B). Most of the identified proteins were novel. The vast majority could be assigned and partly characterized based on homology to annotated proteins in the database.

Of the previously identified proteins, GAP 65 was the most dominant [19], identified in 8 of the 10 bands analyzed (n1, n3, n5–10). In addition, we identified GAP 10 [27] in 7 of the bands (n1, n3, n4, n6, n8–10), while CqCDA1 [26] was found in only one band (n10). The most dominant of the novel proteins was named GAP 59, based on its calculated molecular weight. GAP 59 was identified in 8 of the 10 bands (n3–10). Using the SMART algorithm we found that, like GAP 65 [19], GAP 59 is a member of the chitin-deacetylase family of proteins possessing the characteristic set of three domains; chitin-binding domain 2 (ChtBD2, amino-acids 22–80); low-density lipoprotein receptor class A domain (LDLa, amino-acids 97–134); and polysaccharide/chitin deacetylase domain (CDA, amino-acids 169–299) [8]. A chitinase named *C. quadricarinatus* chitinase 2 (CqChitinase2) was identified in 4 bands (n1, n3–5). Chitinases are enzymes that catalyze the cleavage of chitin [9,44]. CqChitinase2 is an endochitinase that cleaves chitin strands internally, releasing multimers of low molecular mass. Two bands (n1 and n3) contained the enzyme beta-N-acetylglucosaminidase. Previous studies attribute two different potential activities for beta-N-acetylglucosaminidases in chitin structure assembly; 1) generating N-acetylglucosamine monomers from low molecular mass multimers as exochitinases, as was suggested for fungal chitin assembly [44], or 2) modification of cuticular glycoproteins and onset of mineralization, as was suggested from experimental work on the cuticles of the blue crab *Callinectes sapidus* [6,45–47]. Another potentially chitin-binding protein identified was designated as GAMP-like (n3, n5, n7–10), based on its similarity in sequence to the *P. clarkii* gastrolith matrix protein [GAMP, 30, 31] (Fig. 4), which is a strong chitin-binder. Specifically, two factors led to the naming of this novel *C. quadricarinatus* gastrolith matrix protein as GAMP-like. First, 30.7% identity exists between amino acid positions 43–207 of GAMP-like and a region containing several copies of a 10 residue repeat between amino acid positions 64–229 of *P. clarkii* GAMP (Fig. 4, upper panel). In addition, strong similarity in amino acid composition exists in the aligned areas of the two proteins (Fig. 4, lower panel), which consist almost entirely of Gly, Ala, Val, Gln and Glu. However, in contrast to the strong denaturation required for extraction of GAMP from the gastrolith chitin matrix, as reported by Ishii et al. in 1996 [31], GAMP-like is at least partly released from the *C. quadricarinatus* gastrolith matrix during calcium removal, without a requirement for any protein denaturing agent. Another difference between the two proteins lies in their lengths and properties. The GAMP sequence comprises two parts, each featuring distinct amino acid content and a distinct sequence repeat; GAMP-like is significantly shorter and corresponds only to the first part of the GAMP sequence.

C. quadricarinatus chitin-binding protein (CqCBP) was identified in 4 of the bands (n1, n3, n4, n6). This protein contains a chitin-binding 4 domain also known as the Rebers & Riddiford consensus (R&R [48]). In addition, we identified proteins not predicted to bind chitin, yet that may function in chitin modification, namely the 7 CqHc proteins previously identified in the gastrolith matrix (CqHc1, n1–3, n9; CqHc2, n1–3; CqHc3, n1, n2; CqHc4, n3; CqHc5, n1, n3; CqHc6, n3; CqHc7, n3) [29]. In our study of gastrolith hemocyanins, we demonstrated *in vitro* phenoloxidase activity for these proteins, and suggested their involvement in the process of chitin sclerotization during cuticle formation. Besides the known hemocyanins, we identified *C. quadricarinatus* cryptocyanin 1 (CqCc1, n3) which is also a member of the crustacean hemocyanin superfamily but lacks the signature oxygen-binding property. Cryptocyanins are primarily suggested to serve as storage proteins for the newly synthesized cuticle of the molting crustacean [49,50], although other roles have been proposed, including the transport of hemolymph calcium to calcifying tissues, or alternatively, the transport of ecdysone [51,52].

Along with GAP 10, we found two proteins that may be implicated in the process of calcium precipitation (Fig. 5). The first, GAP 18.2 (n4, n7,

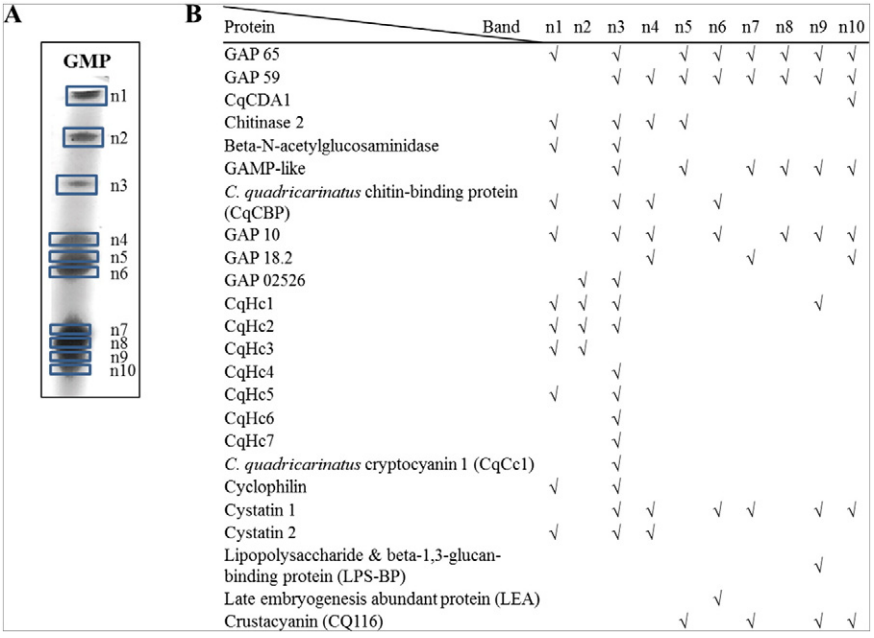

Protein \ Band	n1	n2	n3	n4	n5	n6	n7	n8	n9	n10
GAP 65	√		√		√	√	√	√	√	√
GAP 59			√	√	√	√	√	√	√	√
CqCDA1										√
Chitinase 2	√		√	√	√					
Beta-N-acetylglucosaminidase	√		√							
GAMP-like			√		√		√	√	√	√
C. quadricarinatus chitin-binding protein (CqCBP)	√		√	√		√				
GAP 10	√		√	√		√		√	√	√
GAP 18.2				√			√			√
GAP 02526		√	√							
CqHc1	√	√	√						√	
CqHc2	√	√	√							
CqHc3	√	√								
CqHc4			√							
CqHc5	√		√							
CqHc6			√							
CqHc7			√							
C. quadricarinatus cryptocyanin 1 (CqCc1)			√							
Cyclophilin	√		√							
Cystatin 1			√	√		√	√		√	√
Cystatin 2	√		√	√						
Lipopolysaccharide & beta-1,3-glucan-binding protein (LPS-BP)									√	
Late embryogenesis abundant protein (LEA)						√				
Crustacyanin (CQ116)					√		√		√	√

Fig. 3. Native gel analysis of gastrolith matrix proteins. A) Native PAGE of GMPs. Bands marked with rectangles were excised and analyzed by MS. B) MS identification of the prominent proteins in each excised band.

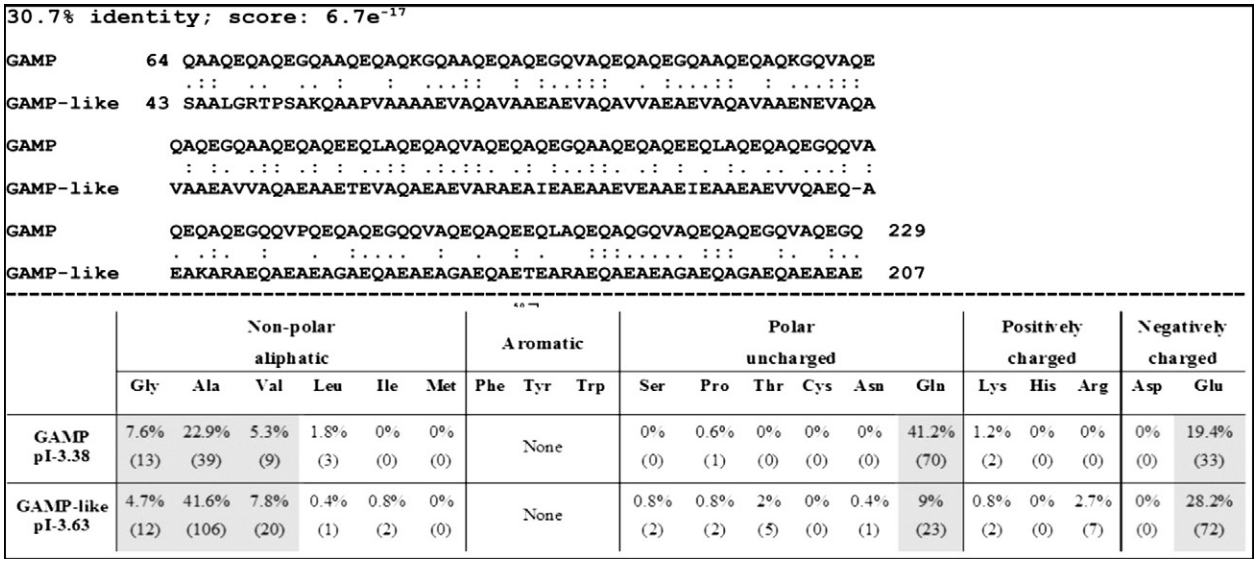

	Non-polar aliphatic						Aromatic			Polar uncharged						Positively charged			Negatively charged	
	Gly	Ala	Val	Leu	Ile	Met	Phe	Tyr	Trp	Ser	Pro	Thr	Cys	Asn	Gln	Lys	His	Arg	Asp	Glu
GAMP pI-3.38	7.6% (13)	22.9% (39)	5.3% (9)	1.8% (3)	0% (0)	0% (0)	None			0% (0)	0.6% (1)	0% (0)	0% (0)	0% (0)	41.2% (70)	1.2% (2)	0% (0)	0% (0)	0% (0)	19.4% (33)
GAMP-like pI-3.63	4.7% (12)	41.6% (106)	7.8% (20)	0.4% (1)	0.8% (2)	0% (0)	None			0.8% (2)	0.8% (2)	2% (5)	0% (0)	0.4% (1)	9% (23)	0.8% (2)	0% (0)	2.7% (7)	0% (0)	28.2% (72)

Fig. 4. Sequence composition similarity between GAMP and GAMP-like. The upper panel shows a comparison of the 10 amino acid-long repeats between positions 64–229 in GAMP with part of the GAMP-like sequence (positions 43–207). Colons indicate identity, while periods indicate conserved replacements. The lower panel shows a comparison of the amino acid compositions of the aligned sequences in the upper panel. Numbers of amino acids corresponding to relative percentages are indicated within brackets. The most abundant amino acids in both proteins are highlighted in gray.

n10), shows significant similarity to GAP 10 (Fig. 5A). GAP 18.2 consists of 188 amino acids, with the first 15 predicted to be a signal peptide by the SignalP 3.0 server (Fig. 5A, upper panel). Bioinformatics searches did not detect known chitin-binding domains or any other domains found in previously published gastrolith proteins, such as LDLa and CDA. Alignment of the entire mature sequences (i.e. without the signal peptides) of GAP 10 and GAP 18.2 revealed 42.2% identity between GAP 10 amino acids 17–113 and GAP 18.2 amino acids 31–132, with a score of $9.3e^{-18}$ (Fig. 5A, lower panel). In addition, outside of this high sequence identity region, GAP 18.2 and GAP 10 share additional consensus sequences found in arthropod cuticular proteins [53], such as AAP(A/V) repeats, present upstream of the high sequence identity region (GAP 18.2 residues 39–42 and 49–52), and glycine-rich GGX repeats (GAP 18.2 residues 58–60).

The second protein potentially involved in calcium precipitation is the partial sequence named GAP 02526 (n2, n3) which could not be annotated relying of the available known protein database but contains high percentages of Gln (9.5%), Glu (15.8%), Pro (11.1%), Ser (11.1%), Thr (8.4%) and Val (9.5%) (Fig. 5B) and has a calculated pI of 3.57. Such composition is also seen in several proteins extracted from calcium carbonate precipitations in other invertebrate groups, such as echinoderms [54–56], mollusks [57–60] and also ascidians [61].

Another group of proteins identified are those suggested to be involved in the immune response, including a cyclophilin, two cystatins and a lipopolysaccharide and beta-1,3-glucan-binding protein (LPS-BP). Cyclophilin (n1, n3) belongs to a family of proteins found in all living organisms, and exhibit peptidyl-prolyl *cis–trans* isomerase activity during protein folding [62,63]. Cyclophilins are diverse in their subcellular localizations, and include secretion pathway-targeted members, such as the presently identified gastrolith cyclophilin. In the horseshoe crab, a marine arthropod, a 27 kDa protein designated cyclophilin G was identified in hemocyte secretory granules containing antimicrobial peptides that undergo exocytosis upon stimulation by bacterial-derived substances [64]. Apart from a strong similarity to cyclophilin B, the horseshoe crab protein also exhibited isomerase activity.

Two cystatin sub-types, cystatin 1 (n3, n4, n6, n7) and cystatin 2 (n1, n3, n4) were identified. Cystatins are a family of competitive cysteine

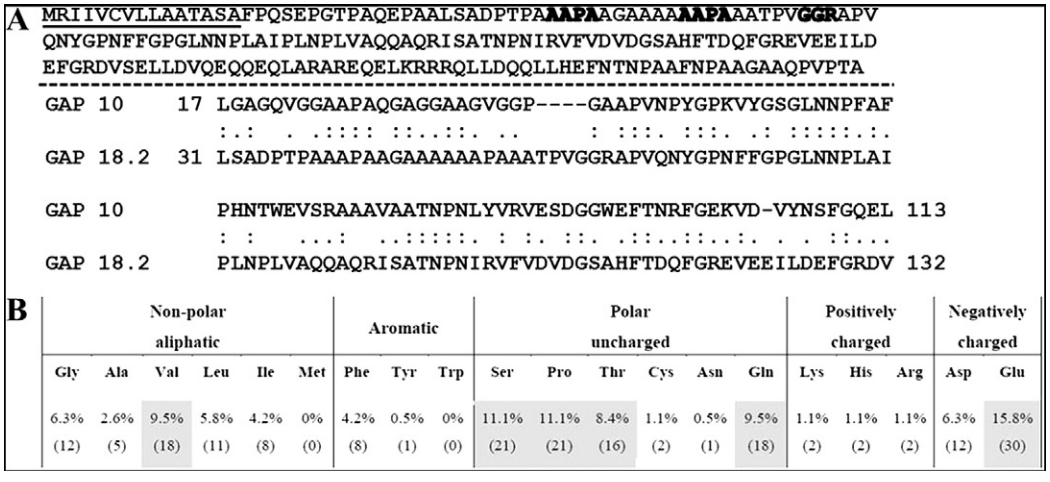

	Non-polar aliphatic						Aromatic			Polar uncharged						Positively charged			Negatively charged	
	Gly	Ala	Val	Leu	Ile	Met	Phe	Tyr	Trp	Ser	Pro	Thr	Cys	Asn	Gln	Lys	His	Arg	Asp	Glu
	6.3% (12)	2.6% (5)	9.5% (18)	5.8% (11)	4.2% (8)	0% (0)	4.2% (8)	0.5% (1)	0% (0)	11.1% (21)	11.1% (21)	8.4% (16)	1.1% (2)	0.5% (1)	9.5% (18)	1.1% (2)	1.1% (2)	1.1% (2)	6.3% (12)	15.8% (30)

Fig. 5. Properties and analysis of proteins putatively involved in calcium precipitation. A) The deduced sequence of GAP 18.2 and sequence conservation of GAP 10 and GAP 18.2 are shown. In the upper panel, the deduced protein sequence of GAP 18.2 is given. The predicted signal peptide is underlined, and the consensus sequences (AAP(A/V) and GGX repeats) are outlined. In the lower panel, alignment of GAP 10 amino acids 17-113 and GAP 18.2 amino acids 31-132 is provided. Colons indicate identity, while periods indicate conserved replacements. B) The deduced amino acid composition of GAP 02526. Numbers of amino acids corresponding to relative percentages are indicated within brackets. The most abundant amino acids in both proteins are highlighted in gray.

proteinase inhibitors ubiquitously present in vertebrates, invertebrates and plants [65]. Cystatins are known to have anti-fungal, anti-viral and anti-bacterial activities, serving regulatory roles for both endogenous and exogenous cysteine proteinases. Although our library sequence does not cover the entire transcript, cystatin 1 contains one copy of the cystatin-like domain, while cystatin 2 contains at least 4 repeats of this motif. LPS-BP was found only in band n9. The crustacean lipopolysaccharide and beta-1,3-glucan binding proteins, also named coelomic cytolytic factors, are a subgroup of glycoside hydrolase family 16 that form complexes with pathogen-associated beta-1,3-glucans which then activate prophenoloxidases and other immune factors [66].

We additionally identified a late embryogenesis abundant protein (LEA, n6) found to protect other proteins from aggregation in the face of extreme conditions, such as osmotic stress [67–69], and a crustacyanin (CQ116, n5, n7, n9, n10) which is a strictly crustacean protein belonging to the superfamily of lipocalins [11]. Crustacyanins form multimeric complexes with the carotenoid astaxanthin, giving rise to the familiar shell coloration of malacostracan crustaceans (including crayfish) [11]. The presence of crustacyanin in *C. quadricarinatus* gastroliths is puzzling, since they lack coloration, although gastroliths of other crayfish species, such as *P. clarkii*, are blue [70].

3.4. Cross-linking and 2D-electrophoretic analysis of gastrolith matrix proteins for defining protein complex composition

With the aim of identifying complexes formed by the above-listed proteins, we subjected GMPs to a cross-linking treatment, followed by 2D-electrophoretic separation (see Materials and methods). For cross-linking, we used FA due to three important properties [38]. First, FA possesses the shortest possible spacer arm, forming cross-bridges between molecules that are necessarily in very close proximity (2.3–2.7 Å), a characteristic of protein complexes [38]. Second, the cross-linking reaction rate of FA is very high, enabling it to capture short-lived protein complexes. Third, FA-mediated cross-linking is reversible. In 2D-PAGE, proteins that are not part of a complex created a diagonal line, as seen in Fig. 6A. However, proteins held together by FA cross-linking bridges were separated only in the second PAGE, and, therefore, appear in Fig. 6A as bands below the diagonal line.

Four putative complexes (a–d) were identified, all containing both GAP 65 and cystatin 2 (Fig. 6B). Complex a consisted of GAP 65, GAP 59, cystatin 2, CqHc1–3, GAP 10 and GAP 02526. Complex b consisted of only GAP 65, cystatin 2 and CqHc2. Complex c consisted of GAP 65 and GAP 59, cystatin 2, CqHc1–5, GAMP-like, GAP 10 and beta-N-acetylglucosaminidase. Finally, complex d consisted of GAP 65 and GAP 59, cystatin 2, CqHc1, GAMP-like, LPS-BP, CqCBP and LEA.

3.5. Identifying candidates in direct association with GAP 65

Since GAP 65 was found to be present in most of the native bands and in all of the putative complexes, we next considered which proteins would be most likely to be in direct contact with GAP 65. Accordingly, we introduced biotinylated purified native GAP 65 to a GMP solution, followed by avidin precipitation, SDS-PAGE and MS analysis of three distinct bands excised from the gel (Fig. 7A; AP1, AP2, AP3). Fig. 7B shows that GAP 65 was identified in all three precipitated bands along with GAMP-like. AP2 consists of GAP 65 and GAMP-like alone. However, AP1 and AP3 also contain GAP 59 and GAP 10, as well as several band-specific proteins. Since all of the proteins found in the avidin precipitation assay were already identified in the previous assays, these results reconfirm our above findings.

3.6. Putative complexes and interactions among gastrolith matrix proteins

Through integration of the results of our biochemical assays, we propose three chief complexes formed by GMPs (Fig. 8). The compositions of complexes I, II and III were determined by focusing on proteins that are unique to each of the complexes d, c and a, respectively, from the cross-link/2D-PAGE experiment and relating them to the results provided by native PAGE. Proteins found in complex with a unique protein according to the cross-link/2D experiment and also identified in the same band by native PAGE were deemed to be part of the same complex.

The components of the three complexes identified in this manner are schematically depicted in Fig. 8. GAP 65 is positioned at the top of each complex, with associated proteins captured by avidin precipitation placed directly below and marked by asterisks. Each protein was then colored according to its putative function, such as chitin binding, chitin modification and calcium precipitation. It should be noted that in order

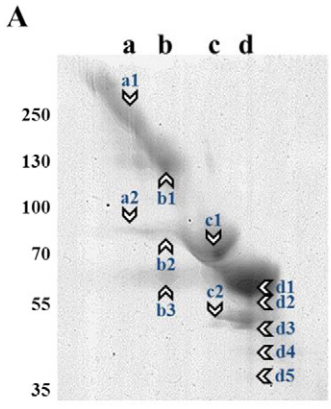

B

Protein \ Band	Complex a		Complex b			Complex c			Complex d				
	a1	a2	b1	b2	b3	c1	c2	c3	d1	d2	d3	d4	d5
GAP 65	√		√		√	√	√		√	√			√
GAP 59	√						√			√			
Beta-N-acetylglucosaminidase						√							
GAMP-like								√			√		
CqCBP										√			
GAP 10	√					√							
GAP 02526	√												
CqHc1	√	√				√				√			
CqHc2	√	√		√		√							
CqHc3		√				√							
CqHc4						√							
CqHc5						√							
Cystatin 2	√		√			√				√			
LPS-BP										√		√	
LEA												√	

Fig. 6. Identification of protein complexes in the gastrolith matrix. A) 2D SDS-PAGE separation of GMPs. The first dimension of separation was performed following cross-linking using FA. The second dimension of separation was performed following heating in denaturizing solution. Bands appearing under the diagonal line correspond to proteins that are part of complexes (a, b, c, and d represent distinct protein complexes). B) MS identification of the prominent proteins in each complex.

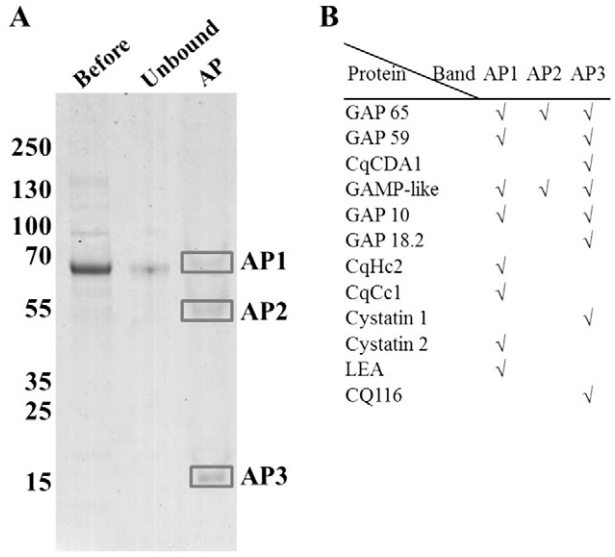

Fig. 7. Identification of gastrolith matrix proteins potentially interacting with GAP 65 using an avidin-precipitation assay. A) SDS-PAGE of biotinylated GAP 65 precipitation with agarose-bound streptavidin. B) MS identification of GAP 65 and co-precipitated proteins in each rectangularly marked band. AP, avidin precipitation.

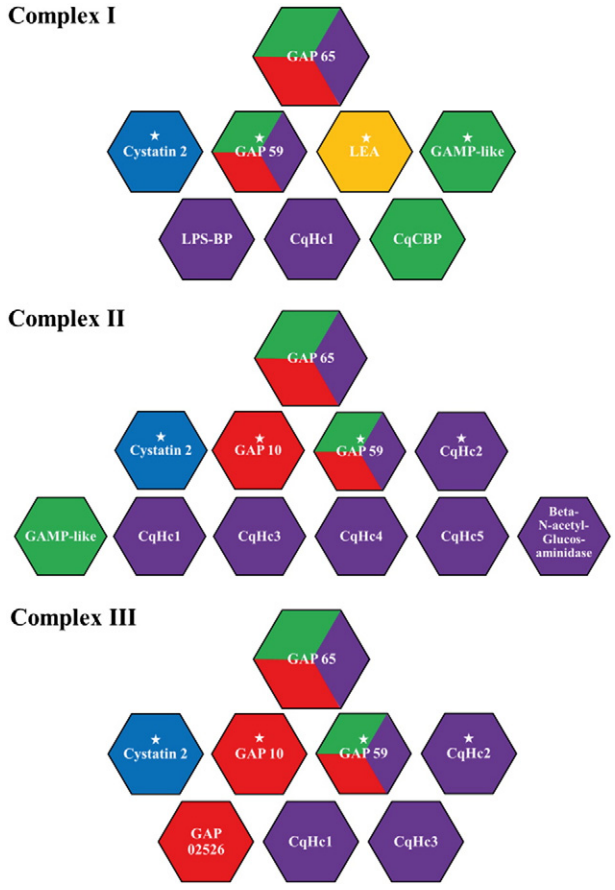

Fig. 8. Proposed protein complexes as identified by both 2D SDS-PAGE and native PAGE. Complex I is based on 2D PAGE complex d, complex II is based on 2D PAGE complex c, and complex III is based on 2D PAGE complex a. Asterisks indicate proteins that are likely to be directly associated with GAP 65, according to the avidin precipitation assay. Hexagon colors indicate putative function based on protein domains as predicted by the SMART algorithm and our sequence analysis; green — chitin-binding, purple — chitin modification, red — calcium-binding, blue — immune response, and yellow — protein stability.

to establish the specific direct associations of proteins not marked by asterisks to the suggested complexes and the functionality of these associations, further studies will be required.

We view the complexes suggested in Fig. 8 as being the dominant forms of a highly dynamic process, in which a few proteins (GAP 65, GAP 59, cystatin2 and CqHc1) remain constant and other participating proteins assemble and disassemble in a given order. Therefore, we propose a sequence of events for the involvement of the three protein complexes in a dynamic cycle of chitin assembly and calcification. Complex I serves as an initiator of chitin network formation, since it contains chitin-binding and chitin-interacting/remodeling proteins, as well as the protein-stabilizing LEA protein and the proteinase inhibitor cystatin 2. Replacing some complex I proteins, such as LEA, CqCBP and LPS-BP, by hemocyanins and beta-N-acetylglucosaminidase, yields complex II. This complex is proposed to be involved in remodeling of the forming chitin network and contributes to its sclerotization. Furthermore, the presence of beta-N-acetylglucosaminidase suggests that complex II might also be involved in initiation of calcification. The cycle is complete when complex II is converted into complex III by shedding most of the chitin-manipulating proteins and recruiting proteins that are involved in calcium carbonate precipitation, such as GAP 10 and possibly GAP 02526.

To our knowledge, this is the first study identifying the presence and composition of protein complexes in an invertebrate cuticular structure. To determine the exact sequence of events and the factors involved, additional research is required. Yet, based on the findings reported here, together with our earlier results concerning gastrolith structure and assembly, we propose a summarizing model [12,17,19,27,29] (Fig. 9). The model focuses on small-scale close interactions that occur immediately on the inner surface of the GFE that is lined by secreting microvilli, and presents a hypothesis for a cyclic process by which layers of chitin–protein–mineral are formed.

To describe these interactions, we first present an H&E-stained cross section of a decalcified gastrolith pouch, in which the interface area between the tissue (at the apical face of the epithelial cells) and the gastrolith matrix is indicated (Fig. 9A, rectangle with dashed lines). This image shows that the microvilli are directly attached to the matrix. Next, we created a cartoon reproduction of a simplified magnification of the interface area (Fig. 9B), where we simplified the epithelial microvilli by reducing their lengths, abundance and folding, and also simplified the gastrolith matrix so that the chitin strands and the ACC spherules can be readily seen. Our illustration of the epithelial microvilli is based on TEM images of the GFE, such as those in Fig. 3. The illustration of the matrix chitin strands and ACC spherules is based on high resolution scanning electron microscope images, as presented in a previous paper [12]. GMP complexes are also incorporated into the model in Fig. 9C, where the cartoon images show a higher magnification of the area where the microvilli contact the forming matrix.

The left panel of Fig. 9 describes the first stage of the gastrolith matrix-forming cycle, reflecting three activities: 1) on the plasma membrane, membrane-bound chitin synthase assembles new chitin strands (Fig. 9C, black ovals) [71]. Merzendorfer & Zimoch [1] suggested several alternative models for chitin formation in insects that may also apply to crustaceans. In the more widely accepted model, chitin synthase is transported to the plasma membrane in intracellular vesicles in an inactive form. There, it is activated after membrane fusion when facing the extracellular space. 2) Within the microvilli cytoplasm, transport vesicles advance to the secreting apical face of the epithelial cells. These vesicles contain various GMPs (Fig. 9C, multi-colored hexagons) required for the assembly of complex I. 3) Copies of complex I are attached to the assembling chitin strands (Fig. 9C, white hexagons). This complex contains chitin-binding and chitin-interacting/remodeling proteins, as well as the protein-stabilizing LEA protein and the proteinase inhibitor cystatin 2. We propose that complex I is the first dominant protein assembly in the cycle, serving as an initiator of chitin network formation.

The middle panel describes the next stage in which some complex I proteins, such as LEA, CqCBP and LPS-BP, are replaced by hemocyanins

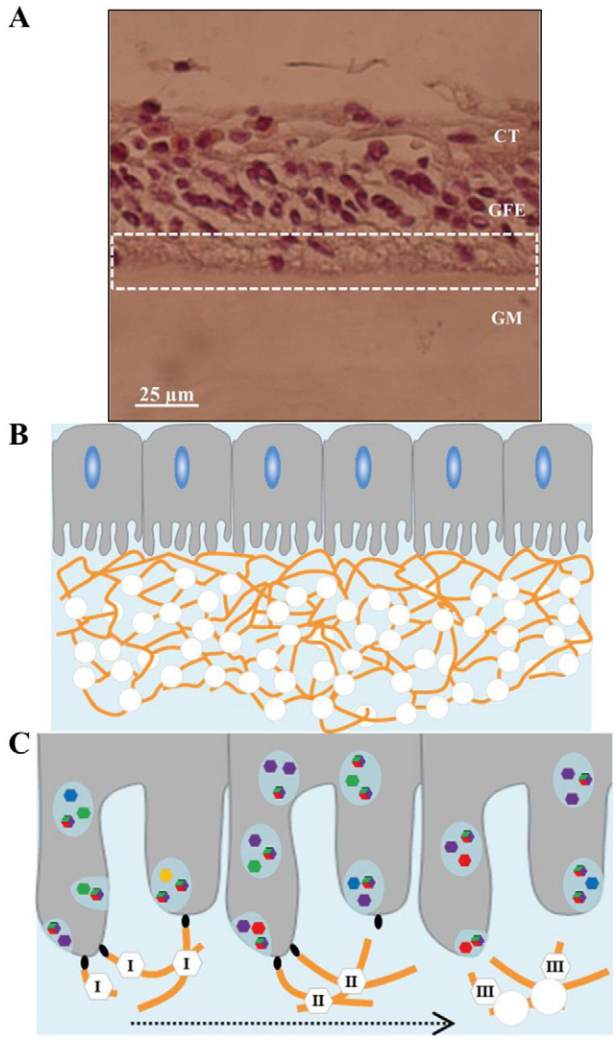

Fig. 9. A model for the involvement of the putative complexes I, II and III in the assembly of the gastrolith chitinous matrix and in deposition of ACC. A) H&E staining of a cross-section of a partially decalcified gastrolith pouch. The dashed rectangle indicates the interface between the gastrolith-forming epithelium (GFE) and the gastrolith matrix (GM). CT, connective tissue. B) Hypothetical illustration of the interface area indicated in A. C) Illustration of a higher magnification of the interface area showing secretion of chitin, synthesized by membrane-bound chitin synthetases (black ovals), secretion vesicles containing GMPs (multi-colored hexagons), and protein complexes (white hexagons). Left image: Complex I is involved in formation of the chitin network. Middle image: Complex II is involved in sclerotization of the chitin network. Right image: Complex III is involved in deposition of the ACC. The dashed arrow indicates cycle direction.

and beta-N-acetylglucosaminidase, to yield complex II. This complex remodels the forming chitin network and contributes to its sclerotization. Finally, the right panel describes the last stage of the cycle, in which complex II is converted into complex III by shedding most of the chitin-manipulating proteins and recruiting proteins that are involved in calcium carbonate precipitation, such as GAP 10 and possibly GAP 02526.

Our model describes one cycle in a continuous process consisting of numerous cycles that occur simultaneously along the epithelium–matrix interaction surface where layers of chitin–protein–mineral are formed. The main 'players' operating in this process are the three identified protein complexes. The presence of GAP 65 in all three complexes coincides with its dominant abundance in the gastrolith, as shown in Fig. 1. Moreover, our suggestion that complex members are transported to the extracellular matrix via secretion vesicles is supported by the evidence presented in Fig. 2, showing GAP 65 associated with intracellular membranes suspected as being secretion pathway elements.

4. Concluding remarks

A deeper understanding of the calcified crustacean exoskeleton structure, as well as the processes of exoskeleton construction and replacement during the molt cycle, can answer many biological questions and promote numerous biotechnological developments. In the present study, we combined data from our recently established *C. quadricarinatus* epithelial transcriptome library [29] with new data collected by tandem MS analyses of gastrolith protein extracts. Accordingly, we have identified a set of novel *C. quadricarinatus* gastrolith matrix proteins, that, when combined with the list of previously identified proteins, offer a near-complete and comprehensive picture of the gastrolith proteome. Furthermore, using various biochemical approaches, we also obtained strong evidence for their association into complexes.

Shechter et al. previously defined the dual role of GAP 65 in forming the chitinous scaffold of the gastrolith and in depositing ACC [19]. In the present study, we considered the molecular mechanism behind this dual function, suggesting a coordinating role for GAP 65 with other proteins fulfilling the different functions required.

Finally, we propose a hypothetical model which integrates relevant evidence that was accumulated up to this point into a probable sequence of events leading to the formation of a relatively simple cuticular structure, such as the gastrolith. While the model suggests protein–protein, protein–chitin and protein–mineral interactions, further studies are required to elucidate each such interaction.

Acknowledgments

We thank Mr. Aviv Ziv, Mr. Tom Levi and Mr. Omri Lapidot for technical assistance. We thank Ms. Ayana Benet Perlberg of the Dor Agriculture Center, Department of Fisheries and Aquaculture, Israel Ministry of Agriculture and Rural Development, for the supplied animals. We thank Dr. Eyal Gur for assistance in creating the cartoon model. We thank Ms. Rina Jeger for the assistance in gastrolith tissue cryosectioning, GAP 65 immunolabeling and TEM imaging. This work was supported by the Israel Science Foundation (ISF grant no. 102/09).

Appendix A. Supplementary data

Supplementary data to this article can be found online at http://dx.doi.org/10.1016/j.jprot.2015.08.016.

References

[1] H. Merzendorfer, L. Zimoch, Chitin metabolism in insects: structure, function and regulation of chitin synthases and chitinases, J. Exp. Biol. 206 (2003) 4393–4412.
[2] K.M. Rudall, W. Kenching, The chitin system, Biol. Rev. Camb. Philos. Soc. 49 (1973) 597–636.
[3] F.G. Carey, Chitin synthesis *in vitro* by crustacean enzymes, Comp. Biochem. Physiol. 16 (1965) 155–158.
[4] J. Blackwell, M.A. Weih, Structure of chitin–protein complexes — ovipositor of the ichneumon fly *Megarhyssa*, J. Mol. Biol. 137 (1980) 49–60.
[5] E. Cohen, Chitin synthesis and inhibition: a revisit, Pest Manag. Sci. 57 (2001) 946–950.
[6] A.V. Kuballa, A. Elizur, Differential expression profiling of components associated with exoskeletal hardening in crustaceans, BMC Genomics 9 (2008) 575.
[7] H.A. Lowenstam, S. Weiner, On Biomineralization, Oxford University Press, New-York, 1989.
[8] R. Dixit, Y. Arakane, C.A. Specht, C. Richard, K.J. Kramer, R.W. Beeman, et al., Domain organization and phylogenetic analysis of proteins from the chitin deacetylase gene family of *Tribolium castaneum* and three other species of insects, Insect Biochem. Mol. Biol. 38 (2008) 440–451.
[9] Y. Arakane, S. Muthukrishnan, Insect chitinase and chitinase-like proteins, Cell. Mol. Life Sci. 67 (2010) 201–216.
[10] R.D. Rosa, M.A. Barracco, Antimicrobial peptides in crustaceans, Invertebr. Surviv. J. 7 (2010) 262–284.
[11] N.M. Wade, A. Tollenaere, M.R. Hall, B.M. Degnan, Evolution of a novel carotenoid-binding protein responsible for crustacean shell color, Mol. Biol. Evol. 26 (2009) 1851–1864.
[12] L. Glazer, A. Sagi, On the involvement of proteins in the assembly of the crayfish gastrolith extracellular matrix, Invertebr. Reprod. Dev. 56 (2012) 57–65.
[13] S. Jasrapuria, Y. Arakane, G. Osman, K.J. Kramer, R.W. Beeman, S. Muthukrishnan, Genes encoding proteins with peritrophin A-type chitin-binding domains in

Tribolium castaneum are grouped into three distinct families based on phylogeny, expression and function, Insect Biochem. Mol. Biol. 40 (2010) 214–227.
[14] J.H. Willis, Structural cuticular proteins from arthropods: annotation, nomenclature, and sequence characteristics in the genomics era, Insect Biochem. Mol. Biol. 40 (2010) 189–204.
[15] K. Adachi, H. Endo, T. Watanabe, T. Nishioka, T. Hirata, Hemocyanin in the exoskeleton of crustaceans: enzymatic properties and immunolocalization, Pigment Cell Res. 18 (2005) 136–143.
[16] S.O. Andersen, Insect cuticular sclerotization: a review, Insect Biochem. Mol. Biol. 40 (2010) 166–178.
[17] A. Shechter, A. Berman, A. Singer, A. Freiman, M. Grinstein, J. Erez, et al., Reciprocal changes in calcification of the gastrolith and cuticle during the molt cycle of the red claw crayfish *Cherax quadricarinatus*, Biol. Bull. (Woods Hole) 214 (2008) 122–134.
[18] G. Luquet, F. Marin, Biomineralisations in crustaceans: storage strategies, Comp. Rend. Palev. 3 (2004) 515–534.
[19] A. Shechter, L. Glazer, S. Chaled, E. Mor, S. Weil, A. Berman, et al., A gastrolith protein serving a dual role in the formation of extracellular matrix containing an amorphous mineral, Proc. Natl. Acad. Sci. U. S. A. 105 (2008) 7129–7134.
[20] J. Aizenberg, G. Lambert, L. Addadi, S. Weiner, Stabilization of amorphous calcium carbonate by specialized macromolecules in biological and synthetic precipitates, Adv. Mater. 8 (1996) 222–226.
[21] A. Al-Sawalmih, C.H. Li, S. Siegel, H. Fabritius, S.B. Yi, D. Raabe, et al., Microtexture and chitin/calcite orientation relationship in the mineralized exoskeleton of the American lobster, Adv. Funct. Mater. 18 (2008) 3307–3314.
[22] J.R. Clarkson, T.J. Price, C.J. Adams, Role of metastable phases in the spontaneous precipitation of calcium-carbonate, J. Chem. Soc. Faraday Trans. 88 (1992) 243–249.
[23] E. Loste, R.M. Wilson, R. Seshadri, F.C. Meldrum, The role of magnesium in stabilising amorphous calcium carbonate and controlling calcite morphologies, J. Cryst. Growth 254 (2003) 206–218.
[24] R. Roer, R. Dillaman, The structure and calcification of the crustacean cuticle, Am. Zool. 24 (1984) 893–909.
[25] D.F. Travis, The deposition of skeletal structures in the crustacea. 1. The histology of the gastrolith skeletal tissue complex and the gastrolith in the crayfish, *Orconectes* (*cambaus*) *verilis* Hagen — Decapoda, Biol. Bull. (Woods Hole) 16 (1960) 137–149.
[26] Y. Yudkovski, L. Glazer, A. Shechter, R. Reinhardt, V. Chalifa-Caspi, A. Sagi, et al., Multi-transcript expression patterns in the gastrolith disk and the hypodermis of the crayfish *Cherax quadricarinatus* at premolt, Comp. Biochem. Physiol. Part D: Genom. Proteom. 5 (2010) 171–177.
[27] L. Glazer, A. Shechter, M. Tom, Y. Yudkovski, S. Weil, E.D. Aflalo, et al., A protein involved in the assembly of an extracellular calcium storage matrix, J. Biol. Chem. 285 (2010) 12831–12839.
[28] D.F. Travis, The deposition of skeletal structures in the crustacea. 2. The histochemical changes associated with the development of the nonmineralized skeletal components of the gastrolith discs of the crayfish, *Orconectes virilis hagen*, Acta Histochem. 15 (1963) 251–268.
[29] L. Glazer, M. Tom, S. Weil, Z. Roth, I. Khalaila, B. Mittelman, et al., Hemocyanin with phenoloxidase activity in the chitin matrix of the crayfish gastrolith, J. Exp. Biol. 216 (2013) 1898–1904.
[30] K. Ishii, N. Tsutsui, T. Watanabe, T. Yanagisawa, H. Nagasawa, Solubilization and chemical characterization of an insoluble matrix protein in the gastroliths of a crayfish, *Procambarus clarkii*, Biosci. Biotechnol. Biochem. 62 (1998) 291–296.
[31] K. Ishii, T. Yanagisawa, H. Nagasawa, Characterization of a matrix protein in the gastroliths of the crayfish *Procambarus clarkii*, Biosci. Biotechnol. Biochem. 60 (1996) 1479–1482.
[32] N. Tsutsui, K. Ishii, Y. Takagi, T. Watanabe, H. Nagasawa, Cloning and expression of a cDNA encoding an insoluble matrix protein in the gastroliths of a crayfish, *Procambarus clarkii*, Zool. Sci. (Tokyo) 16 (1999) 619–628.
[33] J. Schultz, F. Milpetz, P. Bork, C.P. Ponting, SMART, a simple modular architecture research tool: identification of signaling domains, Proc. Natl. Acad. Sci. U. S. A. 95 (1998) 5857–5864.
[34] J.R. Yates, C.I. Ruse, A. Nakorchevsky, Proteomics by mass spectrometry: approaches, advances, and applications, Annu. Rev. Biomed. Eng. 11 (2009) 49–79.
[35] A. Shechter, M. Tom, Y. Yudkovski, S. Weil, S.A. Chang, E.S. Chang, et al., Search for hepatopancreatic ecdysteroid-responsive genes during the crayfish molt cycle: from a single gene to multigenicity, J. Exp. Biol. 210 (2007) 3525–3537.
[36] K.T. Tokuyasu, A technique for ultracryotomy of cell suspensions and tissues, J. Cell Biol. 57 (1973) 551–565.
[37] U.K. Laemmli, Cleavage of structural proteins during assembly of head of bacteriophage-T4, Nature 227 (1970) 680–685.
[38] B.W. Sutherland, J. Toews, J. Kast, Utility of formaldehyde cross-linking and mass spectrometry in the study of protein–protein interactions, J. Mass Spectrom. 43 (2008) 699–715.
[39] Z. Roth, S. Parnes, S. Wiel, A. Sagi, N. Zmora, J.S. Chung, et al., *N*-glycan moieties of the crustacean egg yolk protein and their glycosylation sites, Glycoconj. J. 27 (2010) 159–169.
[40] X.J. Min, G. Butler, R. Storms, A. Tsang, OrfPredictor: predicting protein-coding regions in EST-derived sequences, Nucleic Acids Res. 33 (2005) W677–W680.
[41] I. Letunic, T. Doerks, P. Bork, SMART 7: recent updates to the protein domain annotation resource, Nucleic Acids Res. 40 (2012) D302–D305.
[42] X.Q. Huang, W. Miller, A time-efficient, linear-space local similarity algorithm, Adv. Appl. Math. 12 (1991) 337–357.
[43] M. Ueno, Calcium-transport in crayfish gastrolith disk — morphology of gastrolith disk and ultrahistochemical demonstration of calcium, J. Exp. Zool. 213 (1980) 161–171.
[44] L. Duo-Chuan, Review of fungal chitinases, Mycopathologia 161 (2006) 345–360.
[45] D.C. Pierce, K.D. Butler, R.D. Roer, Effects of exogenous N-acetylhexosaminidase on the structure and mineralization of the post-ecdysial exoskeleton of the blue crab, *Callinectes sapidus*, Comp. Biochem. Physiol. B Biochem. Mol. Biol. 128 (2001) 691–700.
[46] F.E. Coblentz, T.H. Shafer, R.D. Roer, Cuticular proteins from the blue crab alter in vitro calcium carbonate mineralization, Comp. Biochem. Physiol. Part B: Biochem. Mol. Biol. 121 (1998) 349–360.
[47] R.D. Roer, K.E. Halbrook, T.H. Shafer, Glycosidase activity in the post-ecdysial cuticle of the blue crab, *Callinectes sapidus*, Comp. Biochem. Physiol. B Biochem. Mol. Biol. 128 (2001) 683–690.
[48] J.E. Rebers, J.H. Willis, A conserved domain in arthropod cuticular proteins binds chitin, Insect Biochem. Mol. Biol. 31 (2001) 1083–1093.
[49] N.B. Terwilliger, L. Dangott, M. Ryan, Cryptocyanin, a crustacean molting protein: evolutionary link with arthropod hemocyanins and insect hexamerins, Proc. Natl. Acad. Sci. U. S. A. 96 (1999) 2013–2018.
[50] N.B. Terwilliger, M.C. Ryan, D. Towle, Evolution of novel functions: cryptocyanin helps build new exoskeleton in *Cancer magister*, J. Exp. Biol. 208 (2005) 2467–2474.
[51] N.B. Terwilliger, Gene expression profile, protein production, and functions of cryptocyanin during the crustacean molt cycle, Invertebr. Reprod. Dev. 56 (2011) 229–235.
[52] K.E. van Holde, K.I. Miller, Hemocyanins, Adv. Protein Chem. 47 (1995) 1–81.
[53] R. Futahashi, S. Okamoto, H. Kawasaki, Y.S. Zhong, M. Iwanaga, K. Mita, et al., Genome-wide identification of cuticular protein genes in the silkworm, *Bombyx mori*, Insect Biochem. Mol. Biol. 38 (2008) 1138–1146.
[54] S.C. Benson, N.C. Benson, F. Wilt, The organic matrix of the skeletal spicule of sea urchin embryos, J. Cell Biol. 102 (1986) 1878–1886.
[55] S. Gayathri, R. Lakshminarayanan, J.C. Weaver, D.E. Morse, R.M. Kini, S. Valiyaveettil, *In vitro* study of magnesium-calcite biomineralization in the skeletal materials of the seastar *Pisaster giganteus*, Chemistry 13 (2007) 3262–3268.
[56] S. Raz, P.C. Hamilton, F.H. Wilt, S. Weiner, L. Addadi, The transient phase of amorphous calcium carbonate in sea urchin larval spicules: the involvement of proteins and magnesium ions in its formation and stabilization, Adv. Funct. Mater. 13 (2003) 480–486.
[57] B.A. Gotliv, L. Addadi, S. Weiner, Mollusk shell acidic proteins: in search of individual functions, Chembiochem 4 (2003) 522–529.
[58] B. Marie, G. Luquet, J.P.P. De Barros, N. Guichard, S. Morel, G. Alcaraz, et al., The shell matrix of the freshwater mussel *Unio pictorum* (Paleoheterodonta, Unionoida), FEBS J. 274 (2007) 2933–2945.
[59] L. Pereira-Mouries, M.J. Almeida, C. Ribeiro, J. Peduzzi, M. Barthelemy, C. Milet, et al., Soluble silk-like organic matrix in the nacreous layer of the bivalve *Pinctada maxima*, Eur. J. Biochem. 269 (2002) 4994–5003.
[60] Y. Zhang, L. Xie, Q. Meng, T. Jiang, R. Pu, L. Chen, et al., A novel matrix protein participating in the nacre framework formation of pearl oyster, *Pinctada fucata*, Comp. Biochem. Physiol. Part B: Biochem. Mol. Biol. 135 (2003) 565–573.
[61] J. Aizenberg, G. Lambert, S. Weiner, L. Addadi, Factors involved in the formation of amorphous and crystalline calcium carbonate: a study of an ascidian skeleton, J. Am. Chem. Soc. 124 (2002) 32–39.
[62] R. Miele, M. Borro, M.L. Mangoni, M. Simmaco, D. Barra, A peptidylprolyl *cis/trans* isomerase from *Xenopus laevis* skin: cloning, biochemical characterization and putative role in the secretion, Peptides 24 (2003) 1713–1721.
[63] F.X. Schmid, L.M. Mayr, M. Mucke, E.R. Schonbrunner, Prolyl isomerases: role in protein folding, Adv. Protein Chem. 44 (1993) 25–66.
[64] Y. Takaki, T. Muta, S. Iwanaga, A peptidyl-prolyl *cis/trans*-isomerase (cyclophilin G) in regulated secretory granules, J. Biol. Chem. 272 (1997) 28615–28621.
[65] A. Kolaczkowska, M. Kolaczkowski, A. Sokolowska, H. Miecznikowska, A. Kubiak, K. Rolka, et al., The antifungal properties of chicken egg cystatin against *Candida* yeast isolates showing different levels of azole resistance, Mycoses 53 (2010) 314–320.
[66] M.M. Roux, A. Pain, K.R. Klimpel, A.K. Dhar, The lipopolysaccharide and beta-1,3-glucan binding protein gene is upregulated in white spot virus-infected shrimp (*Penaeus stylirostris*), J. Virol. 76 (2002) 8978.
[67] S.C. Hand, M.A. Menze, M. Toner, L. Boswell, D. Moore, LEA proteins during water stress: not just for plants anymore, Annu. Rev. Physiol. 73 (2011) 115–134.
[68] A. Tunnacliffe, M.J. Wise, The continuing conundrum of the LEA proteins, Naturwissenschaften 94 (2007) 791–812.
[69] W.W. Wang, B. Meng, W.H. Chen, X.M. Ge, S. Liu, J. Yu, A proteomic study on postdiapaused embryonic development of brine shrimp (*Artemia franciscana*), Proteomics 7 (2007) 3580–3591.
[70] G. Luquet, N. Le Roy, I. Zanella-Cleon, M. Becchi, S. Bucarey, M.S. Fernandez, et al., Characterization of crustacyanin-A2 subunit as a component of the organic matrix of gastroliths from the crayfish *Cherax quadricarinatus*, Mater. Res. Soc. Symp. Proc. 1187 (2009) 69–75.
[71] J. Ruizherrera, V.O. Sing, W.J. Vanderwoude, S. Bartnickigarcia, Microfibril assembly by granules of chitin synthetase, Proc. Natl. Acad. Sci. U. S. A. 72 (1975) 2706–2710.